Neurochemistry International 59 (2011) 297–308

Contents lists available at ScienceDirect

Neurochemistry International

journal homepage: www.elsevier.com/locate/nci

The extrinsic and intrinsic apoptotic pathways are involved in manganese toxicity in rat astrocytoma C6 cells

Agustina Alaimo, Roxana M. Gorojod, Mónica L. Kotler *

Departamento de Química Biológica, Facultad de Ciencias Exactas y Naturales, Universidad de Buenos Aires, C1428EGA Buenos Aires, Argentina

ARTICLE INFO

Article history:
Received 15 April 2011
Received in revised form 30 May 2011
Accepted 1 June 2011
Available online 16 June 2011

Keywords:
C6 cells
Apoptosis
Manganese
Mitochondria
Caspases

ABSTRACT

Manganese (Mn) is a trace element known to be essential for maintaining the proper function and regulation of many biochemical and cellular reactions. However, chronic exposure to high levels of Mn in occupational or environmental settings can lead to its accumulation in the brain resulting in a degenerative brain disorder referred to as Manganism. Astrocytes are the main Mn store in the central nervous system and several lines of evidence implicate these cells as major players in the role of Manganism development. In the present study, we employed rat astrocytoma C6 cells as a sensitive experimental model for investigating molecular mechanisms involved in Mn neurotoxicity. Our results show that C6 cells undergo reactive oxygen species-mediated apoptotic cell death involving caspase-8 and mitochondrial-mediated pathways in response to Mn. Exposed cells exhibit typical apoptotic features, such as chromatin condensation, cell shrinkage, membrane blebbing, caspase-3 activation and caspase-specific cleavage of the endogenous substrate poly (ADP-ribose) polymerase. Participation of the caspase-8 dependent pathway was assessed by increased levels of FasL, caspase-8 activation and Bid cleavage. The involvement of the mitochondrial pathway was demonstrated by the disruption of the mitochondrial membrane potential, the opening of the mitochondrial permeability transition pore, cytochrome c release, caspase-9 activation and the increased mitochondrial levels of the pro-apoptotic Bcl-2 family proteins. In addition, our data also shows for the first time that mitochondrial fragmentation plays a relevant role in Mn-induced apoptosis. Taking together, these findings contribute to a deeper elucidation of the molecular signaling mechanisms underlying Mn-induced apoptosis.

1. Introduction

Manganese (Mn) is an essential trace mineral required for the normal brain development as well as for the proper biochemical and cellular functioning of the central nervous system (CNS) (Aschner et al., 1999). Mn is an important cofactor for a variety of enzymes, such as transferases, hydrolases, lyases, arginase, glutamine synthetase and superoxide dismutase (Roth, 2009; Wedler and Denman, 1984).

Although this metal is required in multiple metabolic functions, chronic exposure to Mn high levels in occupational and environmental settings or disease conditions (hepatic encephalopathy) can lead to its accumulation in the CNS, predominantly in the basal ganglia (Dorman et al., 2006). This turns in decreased dopamine levels which finally triggers cell death, causing a syndrome commonly referred to as Manganism, closely resembling Idiophatic Parkinson's Disease (IPD) at both molecular and clinical levels (Benedetto et al., 2009; Roth, 2009). Patients affected by Manganism exhibit psychological and neurological disturbances. Initial symptoms are of psychiatric nature and include compulsive or violent behavior, emotional instability and hallucinations. Regarding the neurological signs, they involve rigidity, tremor, dystonia and progressive bradykinesia.

Mn exposure represents a significant public health matter due to its employment as a catalyst in countless industrial processes. It is also present in fungicides, fertilizers and as a drinking water purifier (permanganate). In addition, the widespread use of the Mn derivative methyl cyclopentadienyl Mn tricarbonyl (MMT) as an antiknock gasoline agent, represents a potential health risk due to the increased atmospheric Mn levels (Benedetto et al., 2009).

Astrocytes are dynamic and metabolically active cells, which participate in crucial processes in brain metabolism and cell-cell communications in the CNS. Several functions have been attributed to astrocytes including ion homeostasis, glutamate uptake, glutamine release, K^+ and H^+ buffering, synthesis of neurotrophic factors, contribution to the CNS immune system and the

* Corresponding author. Address: Departamento de Química Biológica, Facultad de Ciencias Exactas y Naturales, Universidad de Buenos Aires, Avda. Intendente Güiraldes 2160, Ciudad Universitaria, C1428EGA Buenos Aires, Argentina. Tel./fax: +54 1145763342.

E-mail addresses: agusalaimo@gmail.com (A. Alaimo), roxanagorojod@gmail.com (R.M. Gorojod), kotler@qb.fcen.uba.ar (M.L. Kotler).

0197-0186/$ - see front matter © 2011 Elsevier B.V. All rights reserved.
doi:10.1016/j.neuint.2011.06.001

involvement in the brain physiological antioxidant defense (Nedergaard et al., 2003).

Different lines of evidence suggest astrocytes play a major role in Manganism development. In fact, these cells possess a high affinity transport mechanism for Mn (Aschner et al., 2007) and accumulate this metal by up to 200 times the extracellular concentration, reaching intracellular levels of at least 50–75 μM (Tholey et al., 1988). Once it has been transported into the cell, a 60–70% Mn is readily sequestered by mitochondria through the Ca^{2+} uniporter (for references, see Gunter et al., 2006) while the remaining is localized in the cytosol. It has been suggested that in the mitochondrial matrix, Mn can be oxidized becoming a strong pro-oxidizing agent, Mn^{3+}, thus resulting in the cell components oxidation. The formation and accumulation of a redox-active Mn^{3+} complex in the brain mitochondria could result in Mn toxicity (Gunter et al., 2006).

Several reports propose that Mn neurotoxicity is mainly associated with mitochondrial dysfunction leading to decreased oxidative phosphorylation, increased ROS generation (Gunter et al., 2006; Milatovic et al., 2007) and consequent apoptotic cell death.

Mitochondrial involvement in apoptosis has been well characterized, and it is known to comprise two main events; the pro-apoptotic proteins release from the mitochondrial intermembrane space (IMS) (e.g., cytochrome c, apoptosis-inducing factor, and several pro-caspases) into the cytoplasm (Green and Reed, 1998) and the initiation of a dysfunction program that includes the loss of the proton electromechanical gradient across de inner membrane (IM). Cytochrome c release into the cytosol consequently activates pro-caspase-9 and downstream caspases which have been found to amplify the death process (Budihardjo et al., 1999).

Mn has been found to induce apoptosis in different cell types: human B cells (El Mchichi et al., 2007; Schrantz et al., 1999), HeLa cells (Oubrahim et al., 2001), rat pheochromocytoma (PC12) cells (Hirata, 2002; Ito et al., 2006; Liu et al., 2005; Roth et al., 2000), human neuroblastoma SH-SY5Y cells (Li et al., 2010), NIH3T3 cells (Oubrahim et al., 2002) neural stem cells (Tamm et al., 2008) and rat astrocytes (Kotler et al., 2005; Gonzalez et al., 2008; Yin et al., 2008). However, the underlying molecular mechanism by which Mn promotes apoptosis in astrocytes has not been extensively elucidated yet. Therefore, in the present study, a rat astrocytoma cell line (C6) was selected as an *in vitro* model to investigate the molecular signaling pathways involved in Mn-induced apoptosis.

2. Materials and methods

2.1. Reagents

Dulbecco's modified Eagle's medium (DMEM), manganese chloride, 3-(4,5-dimethyl-thiazol-2-yl)-2,5-diphenyl-tetrazolium bromide (MTT), Neutral Red, glutathione reduced form (GSH), N-acetyl-L-cysteine (NAC), melatonin, Hoescht 33258 fluorochrome, 2′,7′-dichlorodihydrofluorescein diacetate (DCDHF-DA), Caspase-3/7 colorimetric substrate acetyl-Asp-Val-Glu-Asp-p-nitroanilide (Ac-DEVD-pNA), ECL detection reagents (luminol and p-coumaric acid) and Bicinchoninic Acid Kit were purchased from Sigma Chemical Co. (St. Louis, MO, USA). Fetal bovine serum (FBS) was obtained from BIO-NOS (Buenos Aires, Argentine). Acetylsalicylic acid was from Bayer (Buenos Aires, Argentine). N-(2-hydroxyethyl)piperazine-N′-(2-ethanesulfonic acid) (HEPES) was from ICN Biomedicals (Irvine, CA, USA). Rabbit polyclonal anti-caspase-8 (H-134): sc-7890 (1:500), PARP-1 (H-250): sc-7150 (1:100), FasL (c-178): sc-6237 (1:300), Bax (N-20):sc-493 (1:500), Bcl-2 (N-19): sc-492 (1:500), mouse polyclonal anti- β- Actin (C4): sc-47778 (1:10000), rabbit IgG-HRP: sc-2030 (1:1000) and mouse IgG-HRP: sc-2031 (1:1000), were purchased from Santa Cruz Biotechnology (Santa Cruz, CA, USA); rabbit anti- caspase-9 (1:500) was from Cell Signaling Technology, Inc. (Danvers, MA, USA); mouse anti- Complex III subunit core 1- OxPhos (1:5000) (Invitrogen Life Technologies, Eugene, Oregon, USA). The mitochondria-specific red fluorescent probe MitoTracker Red CMXRos was from Molecular Probes (Eugene, OR, USA). The specific caspase-3 inhibitor (Ac-DEVD-CMK) and caspase-9 inhibitor III (Ac-LEHD-CMK) were from Calbiochem (San Diego, CA, USA). The specific caspase-8 inhibitor (z-IETD-FMK) was purchased from BD Pharmingen (San Diego, CA, USA). Caspase substrates and inhibitors were dissolved in dimethyl sulfoxide (DMSO). Final concentration of DMSO did not exceed 0.25%. DMSO added to the samples did not affect cell viability, morphology or others parameters tested in this study. All others chemicals used were of the highest purity commercially available.

2.2. Cell culture and treatments

Rat astrocytoma C6 cell line (ATCC® CCL-107™), originally derived from an N-nitrosomethylurea-induced rat brain tumor (Benda et al., 1968), was kindly provided by Dr. Zvi Vogel (Weizmann Institute of Science, Rehovot, Israel). C6 cells were maintained in DMEM supplemented with 10% heat-inactivated FBS, 2.0 mM glutamine, 100 units/ml penicillin, 100 μg/ml streptomycin and 2.5 μg/ml amphotericin B. Cells were cultured at 37 °C in a humidified atmosphere of 5% CO_2–95% air, and the medium was renewed three times a week. For all experiments, C6 cells were removed with 0.25% trypsin, diluted with DMEM 10% FBS and re-plated into 12-well plates (1.2×10^5 cells/well) or 96-well plates (2×10^4cells/well) to yield 70–80% confluent cultures after 24 h. Then, cells were washed with phosphate buffered saline (PBS) and used for exposure studies.

2.3. Nuclear morphology assessment by fluorescence microscopy

Evaluation of nuclear morphology was performed according to Gonzalez et al. (2008). In brief, C6 cells were sub-cultured on glass coverslips in 12-well plates at a density of 6×10^4 cells/ well. After $MnCl_2$ exposure, cells were washed with PBS and fixed with glacial acetic acid: methanol (1:3 v/v) for 10 min at room temperature. Then cells were washed twice with PBS, stained with Hoechst 33258 (1 μg/ml), washed again with PBS and examined under fluorescence microscopy (Eclipse E600, Nikon; Nikon Instech Co., Ltd., Karagawa, Japan) using filters for DAPI (λ_{ex}: 330–380 nm; λ_{em}: 435–485 nm). Images were captured with a CoolPix5000 digital camera (Nikon; Nikon Instech Co., Ltd., Karagawa, Japan). Digital pictures were analyzed and assembled using Adobe Photoshop 7.0 software. Apoptotic cells were scored evaluating the presence of condensed and fragmented nuclei.

2.4. Assessment of cell viability by MTT assay

The 3-(4,5-dimethyl-thiazol-2-yl)-2,5-diphenyl-tetrazolium bromide (MTT) assay was carried out to evaluate cell viability according to the protocol previously described (Mosmann, 1983) with slight modifications (Gonzalez et al., 2008). Briefly, cells were grown in 96-well plates and exposure to $MnCl_2$. Two hours after the end of incubation time, MTT was added to each well to a final concentration of 0.125 mg/ml. Mitochondrial dehydrogenases of viable cells cleave the tetrazolium ring yielding purple formazan crystals. At the end of incubation, formazan was solubilized in 200 μL of DMSO. Absorbance was measured at 570 nm with background subtraction at 655 nm in a BIO-RAD Model 680 Benchmark microplate reader (BIO-RAD laboratories, Hercules, CA, USA) and the MTT reduction activity was expressed as a percentage of the control cells.

2.5. Assessment of cell viability by Neutral Red assay

Neutral Red (NR) retention assay was carried out following the protocol described by Borenfreund and Puerner (1985). This cytotoxicity test is based on the ability of viable cells to incorporate the supravital dye NR in the lysosomes. Following exposure to $MnCl_2$, cells were washed once with PBS and NR solution (50 μg/ml in DMEM) was added to each well. After 2 h incubation at 37 °C, cells were first washed with PBS and then with a 40% formaldehyde:10% $CaCl_2$ solution. Finally, 200 μl of 50% ethanol/1% acetic acid solution were added until complete dissolution was achieved. Absorbance was measured at 570 nm with background subtraction at 690 nm in a BIO-RAD Model 680 Benchmark microplate reader (BIO-RAD laboratories, Hercules, CA, USA). Results were expressed as a percentage of the corresponding control cells.

2.6. Reactive oxygen species generation

Intracellular peroxides were measured by using an oxidation-sensitive fluorescence probe, DCDHF-DA, the oxidized form of which, 2′,7′-dichloro-fluorescein (DCF) is highly fluorescent. After exposure to $MnCl_2$, cells were loaded with 25 μM DCDHF-DA and incubated for 30 min at 37 °C. Then, cells were washed twice with PBS, detached with 50 μl trypsin (0.25%), and diluted with 50 μl PBS. Afterwards, cells were sonicated and cleared by centrifugation (12,000*g*, 20 min, 4 °C). Fluorescence intensity was monitored in the supernatants using a fluorescence spectrometer (LS-50B, Perkin–Elmer, Inc., Wellesley, MA, USA) (λ_{ex}: 490 nm; λ_{em}: 515 nm). Values were normalized to the total amount of proteins determined by the Bicinchoninic Acid Kit.

2.7. Caspases-3/7 activity assay

Caspase activity was measured according to Gonzalez et al. (2008). Briefly, after $MnCl_2$ exposure, C6 cells were washed with PBS and resuspended in lysis buffer (50 mM Tris–HCl buffer pH 7.4, 1 mM EDTA, 10 mM EGTA, 0.01 mM digitonin, 0.5 mM phenylmethylsulfonyl fluoride (PMSF), 1.54 μM aprotinin and 63.86 μM benzamidine) for 30 min at 37 °C. Cell lysates were cleared by centrifugation (12,000*g*, 20 min, 4 °C) and 150 μl of the supernatant (80–100 μg protein) were incubated with 146 μl of incubation buffer (100 mM HEPES pH 7.5, 10% glycerol, 1.0 mM EDTA, 10 mM DTT, 0.5 mM PMSF, 1.54 μM aprotinin and 63.86 μM benzamidine) and 4 μl of the colorimetric substrate for caspase 3/7 (Ac-DEVD-pNA, 100 μM), at 37 °C for 2 h. Blanks were also run containing either the substrate or the cell lysate alone, to deduce in each case. Activity of caspase-3/7 was determined as the release of the chromophore pNA from the substrate measured at 405 nm in a BIO-RAD Benchmark microplate reader (BIO-RAD laboratories, Hercules, CA). Results were expressed as pNA absorbance units per mg protein. Protein concentration was determined according to Bradford (1976).

2.8. Western blots

Western blots were performed according to procedure described by Gonzalez et al. (2008). Immunoreactive bands were detected by chemiluminescence employing ECL detection reagents from Sigma Chemical Co. (St. Louis, MO, USA) and analyzed using the LAS 1000 plus Image Analyzer (Fuji, Tokyo, Japan). Quantitative changes in protein levels were evaluated with ImageJ software (NIH).

2.9. Subcellular fractionation

After $MnCl_2$ treatment, C6 cells were lysed in MSHE buffer (0.22 M mannitol, 0.07 M sucrose, 0.5 mM EGTA, 2 mM HEPES–KOH, pH 7.4) containing protease inhibitors (0.5 mM PMSF, 1.54 μM aprotinin and 63.86 μM benzamidine). The homogenate was centrifuged for 10 min at 700 *g* and the resulting supernatant was centrifuged at 7000 *g* for 20 min to obtain the enriched-mitochondrial pellet. The latter was washed once in 150 mM KCl to deplete mitochondria of surrounding cytosolic mRNAs, and centrifuged at 10,000*g* for 10 min. Finally, the mitochondrial pellet was resuspended in MSHE.

2.10. Analysis of mitochondrial membrane potential

C6 cells (6×10^4 cells/ well) were grown on glass coverslips in 12-well plates. After $MnCl_2$ exposure, cells were washed twice with PBS and incubated with the cell-permeant mitochondria-specific red fluorescent probe MitoTracker Red CMXRos at a final concentration of 75 nM in serum free- culture medium for 30 min at 37 °C. Afterwards, cells were washed twice with PBS and fixed with 4% paraformaldehyde (20 min at room temperature). Finally, cells were washed with PBS and mounted on glass microscope slides. Samples were examined under a Nikon fluorescence microscope Eclipse E600 (Nikon Instech Co., Ltd., Karagawa, Japan) using TRITC filters (λ_{ex}: 528–553 nm; λ_{em}: 600–660 nm). The images were captured with a CoolPix5000 digital camera (Nikon; Nikon Instech Co., Ltd., Karagawa, Japan). Digital pictures were analyzed and assembled using ImageJ software (NIH).

2.11. Statistical analysis

Experiments were carried out at least in triplicate unless otherwise stated.

Results are expressed as mean ± SEM values. Experimental comparisons between treatments were made by Student's *t*-test and one- way ANOVA, followed by Student–Newman–Keuls post hoc test with statistical significance set at $p < 0.05$. All analyses were carried out with GraphPad Prism 4 software (GraphPad Sofware, San Diego, CA, USA).

3. Results

3.1. Manganese induces dose-dependent cytotoxicity

In order to investigate the cytotoxic effects of Mn, C6 astrocytoma cells were exposed to increasing concentrations of $MnCl_2$ (200–1000 μM) for 24 h and cell viability was analyzed employing two distinct methods (MTT and NR) which evaluate different cellular events as mentioned in Section 2.

Over the concentration range analyzed, no cell death was produced by Mn exposure in the presence of 10% SFB (S) (Fig. 1A and B). In contrast, in serum free conditions (SF), a significant Mn concentration-dependent decrease in cell viability was observed, reaching a plateau at Mn 750 μM Mn, producing a 43 ± 3% ($p < 0.001$) and a 60 ± 3% ($p < 0.001$) decrease in cell viability assessed by MTT and NR, respectively. Therefore, we used Mn 750 μM in subsequent experiments to evaluate the molecular mechanisms of cell death in astrocytoma C6 cells.

3.2. Mn induces changes on cell morphology

C6 cells were exposed to $MnCl_2$ (0–750 μM) for 24 h under both S and SF conditions and analyzed by phase-contrast microscopy (Supplementary Fig. 1). Serum-starved C6 cells exposed to Mn exhibited clear morphological changes, becoming rounded, shrunken, and more loosely attached to the bottom of the cell culture dish surface. In addition, membrane blebbing characteristic of the apoptotic cell death was observed (Supplementary Fig. 1c–f). In contrast,

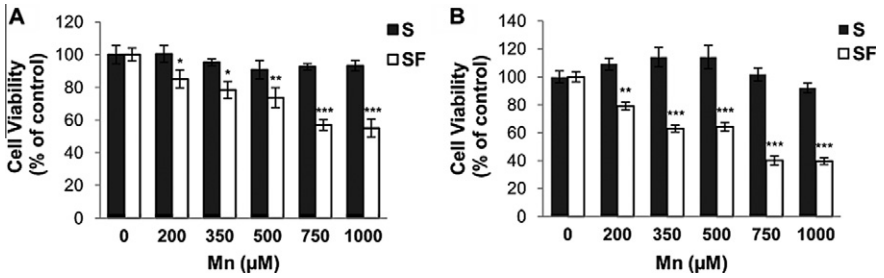

Fig. 1. Mn-induced cytotoxicity. C6 cells were treated for 24 h with 200–1000 μM Mn either in the presence of serum (S) or serum free (SF) and viability was assayed by MTT or Neutral Red. (A) MTT Assay. (B) Neutral Red Assay. Data are expressed as average ± SEM ($n = 8$) and controls are considered 100%. Statistically significant differences between the controls and experimental groups are indicated by: $^{*}p < 0.05$, $^{**}p < 0.01$, $^{***}p < 0.001$ vs. control.

C6 cells incubated with Mn in the presence of serum showed no morphological alterations (Supplementary Fig. 1a and b).

3.3. Manganese-induced cell death is mediated by reactive oxygen species

Increasing evidence indicates that the biological actions of divalent cations are attributable to ROS generation. Even more, it has been demonstrated that Mn induces ROS production in rat primary cortical astrocytes exposed to 1 mM of $MnCl_2$ (Chen and Liao, 2002; Gonzalez et al., 2008). Therefore, to determine whether Mn induces oxidative stress in C6 cells, the changes of the intracellular redox potential after Mn exposure were examined by employing the probe H_2DCF-DA (Fig. 2A). The rate of ROS generation was enhanced by Mn, reaching a 77 ± 4% ($p < 0.001$) increase for 750 μM. Under control conditions, serum deprivation resulted in a non significant 17% increase in ROS production (S: 221.9 ± 1.8; SF: 259.6 ± 5.0 AU/μg protein, $p > 0.05$).

To elucidate whether ROS generation is involved in Mn-induced cell death, the effect of different antioxidants on cell viability was evaluated (Fig. 2B). Pre-incubations with N-acetyl cysteine (NAC, 10 and 20 mM), glutathione (GSH, 0.5 and 1 mM) or acetylsalicylic acid (ASA, 0.1; 1 and 10 mM) prevented Mn-induced cell death in a different extent. However, when cells were pre-treated with melatonin (MLT, 0.001–2 mM) a dual effect could be observed. This neurohormone was able to prevent Mn-induced cell death in pre-incubations at 0.1 and 0.5 mM. In contrast, when C6 cells were exposed to 1 and 2 mM of MLT in the absence of Mn, a significant decrease in cell viability was observed (66 ± 4% and 54 ± 2%, respectively), in accordance with the reported antiproliferative effect of MLT in C6 cells (Martín et al., 2006).

These results provide further evidence about the occurrence of oxidative stress in our experimental model, which seems to play a critical role in the onset of cell death.

3.4. Mn induces apoptotic cell death involving caspase-3 activation and PARP-1 cleavage

To further investigate whether Mn induced-loss of cell viability was attributable to apoptotic cell death, we performed nuclear staining with Hoechst 33258 fluorescent dye to assess changes in nuclear shape and chromatin integrity by fluorescence microscopy (Fig. 3A). In control cultures, nuclei exhibited normal shape and uniformly stained chromatin. However, when cells were exposed to Mn, a 44 ± 7% ($p < 0.001$) of the nuclei showed condensed and

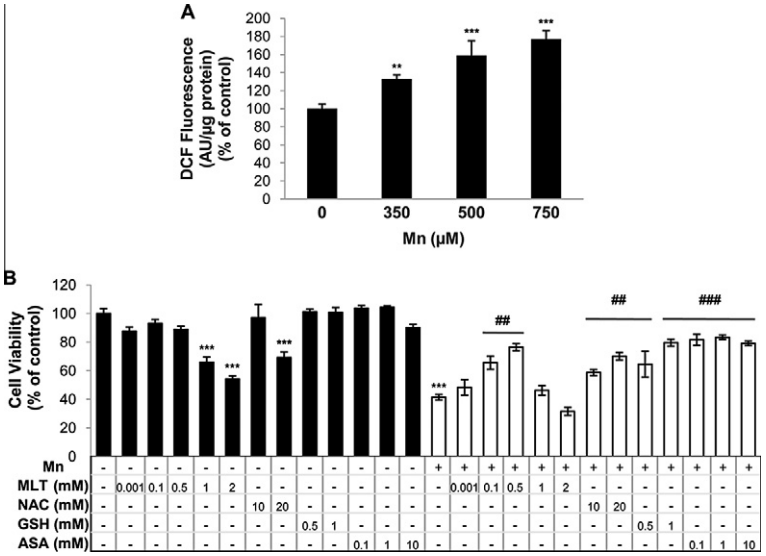

Fig. 2. Mn-induced cell death is mediated by ROS generation. (A) ROS production. After 24 h Mn-treatment under serum free conditions, cells were incubated with DCDHF-DA. The oxidation of the intracellular non-fluorescent DCDHF to highly fluorescent DCF was measured in a fluorescence spectrometer (λ_{exc}: 490 nm; λ_{em}: 515 nm). (B) Protection by antioxidants. C6 cells were pre-incubated for 1 h with melatonin (MLT: 0.001–2.0 mM), N-acetyl cystein (NAC: 10.0 and 20.0 mM), glutathione (GSH: 0.5 and 1.0 mM) and acetylsalicylic acid (ASA: 0.1; 1.0 and 10.0 mM), and then exposed to 750 μM Mn. MTT viability assay was performed. Statistically significant differences between the controls and experimental groups are indicated by: $^{**}p < 0.01$, $^{***}p < 0.001$ vs. control; $^{\#\#}p < 0.01$, $^{\#\#\#}p < 0.001$vs. Mn. AU: arbitrary units.

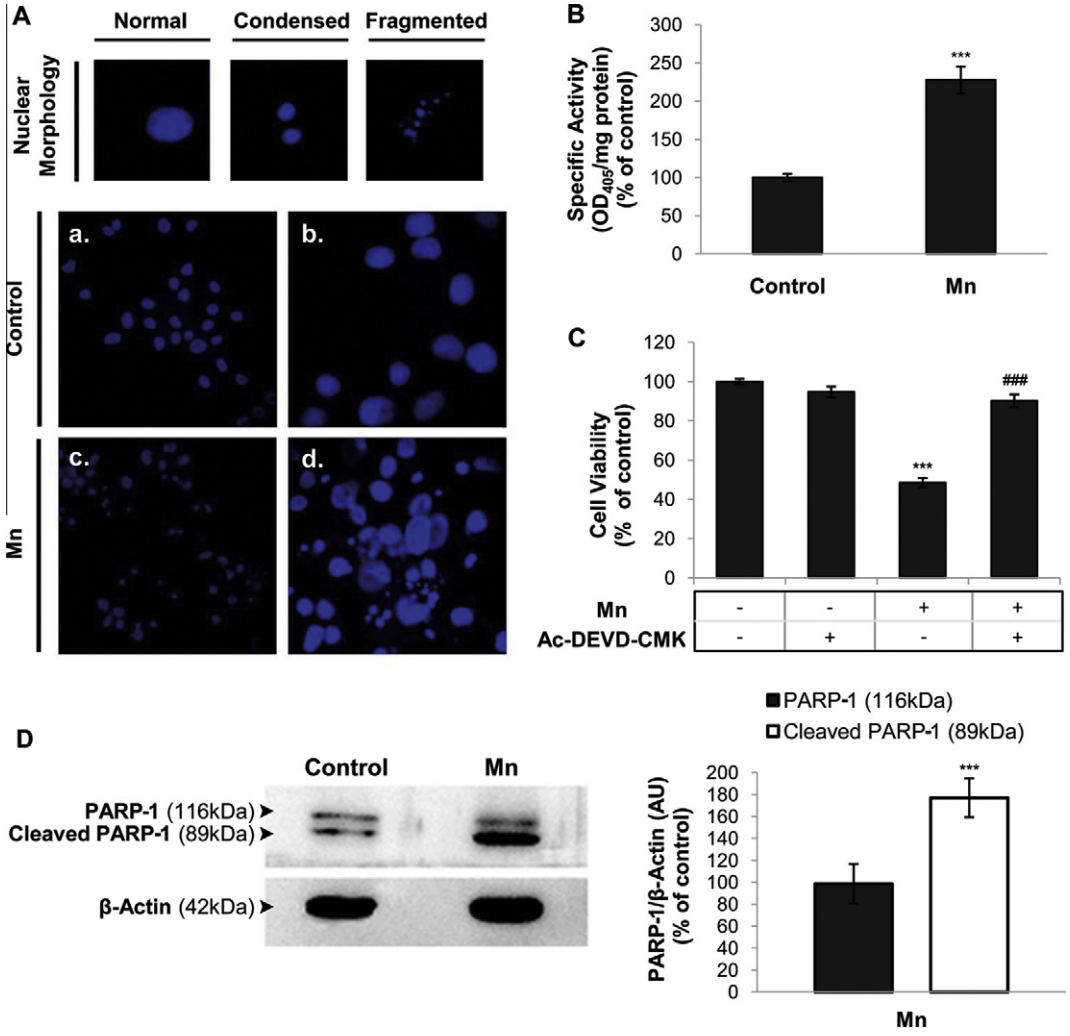

Fig. 3. Mn induces apoptosis in C6 cells. C6 cells were incubated with 750 μM Mn for 24 h under serum free conditions. (A) Nuclear morphology analysis. Nuclear DNA was stained with Hoechst 33258 dye and visualized by fluorescence microscopy using filters for DAPI (λ_{exc}: 330–380 nm; λ_{em}: 435–485 nm). Apoptotic nuclei were visualized as hyper-fluorescent, more condensed and smaller compared to normal nuclei. Control: (a) 400×, (b)1000×; Mn treatment: (c) 400×, (d) 1000×. (B) Caspase 3/7 activity. Specific activity was determined spectrophotometrically using a specific substrate for caspase 3/7 (Ac-DEVD-pNA, 100 mM) and represented as OD_{405}/mg protein. (c) Ac-DEVD-CMK prevents Mn-induced cell death. Cells were incubated for 1 h with 10 μM of caspase-3/7 specific inhibitor (Ac-DEVD-CMK) before Mn treatment. Viability was measured by MTT assay. (D) Mn induces PARP-1 cleavage. A polyclonal antibody that recognizes PARP-1 (116 kDa) and its cleavage product (89 kDa) was used for inmunoblotting analysis. Reprobing with an anti-β-actin antibody was performed to normalize for protein loading. Signals were quantified with the Image J software. Image corresponds to one representative experiment ($n = 3$). Results are expressed as a percentage of the respective control considered as 100%. Statistically significant differences between the controls and experimental groups are indicated by: $^{***}p < 0.001$ vs. control. $^{###}p < 0.001$ vs. Mn. OD: optical density; AU: arbitrary units.

fragmented chromatin, a typical feature of apoptotic cell death, as we previously reported in rat astrocytes (Gonzalez et al., 2008).

It is well known that the initiator and effector caspases, key players that execute the apoptotic cascade, are activated by cleavage in apoptosis (Green and Reed, 1998). Therefore, to determine the possible participation of an apoptotic caspase-dependent pathway in our model, we tested whether Mn exposure activated effector caspases 3/7 and promoted cleavage of the poly(ADP-ribose) polymerase-1 (PARP-1) enzyme, as recently has been demonstrated in cortical astrocytes (Gonzalez et al., 2008). As shown in Fig. 3B, exposure to Mn enhanced caspase 3/7 specific activity 127 ± 17% ($p < 0.001$).

To confirm the engagement of caspase-3 in Mn-induced apoptosis, we pre-incubated C6 cells with the specific inhibitor Ac-DEVD-CMK (10 μM, 1 h) before Mn treatment. In these conditions, a nearly complete recovery in cell viability was detected (90 ± 3%; $p < 0.001$) (Fig. 3C). Cleavage of PARP-1 by effector caspases is one of the markers of cells undergoing apoptosis. We analyzed PARP-1 cleavage in C6 cells exposed to Mn by Western blotting, using an anti-PARP polyclonal antibody which recognizes both the 116- and 89-kDa polypeptides. Fig. 3D shows that PARP-1 is clearly processed 24 h after Mn addition. In fact, cells treated with Mn showed a 77 ± 17% ($p < 0.001$) increase in the 89 kDa PARP-1 levels.

Collectively, these results suggest that Mn induces apoptotic cell death through a caspase-dependent pathway.

3.5. Manganese-induced apoptosis involves caspase-8 activation and Bid cleavage

It is well known that at least two major apoptosis pathways converge on the effector caspases 3/7, the intrinsic (or mitochondrial) and extrinsic (or death receptor) apoptotic pathways (Scaffidi et al., 1998) being caspase-9 and caspase-8, respectively, the apical caspases involved in each pathway.

The intrinsic pathway is activated by a wide range of signals, including oxidative stress induced by Mn (Gonzalez et al., 2008; Yin et al., 2008). In contrast, there are no reports describing the

extrinsic cell death pathway activation in Mn-treated cells. Among the different cell-surface death receptors involved in the extrinsic pathway, Fas plays a relevant role in C6 cells (Saas et al., 1997).

Based on this background and to get deep insight about the apoptotic pathways involved in Mn-induced apoptosis in C6 cells, we analyzed the effect of the specific inhibitors of caspase-8 and caspase-9 (z-IETD-FMK (10 μM) and Ac-LEHD-CMK (10 μM), respectively) on cell viability (Supplementary Fig. 2). Both inhibitors were effective preventing cell death but at a different extent; while a 74 ± 5% ($p < 0.01$) of viability was recovered with Ac-LEHD-CMK, an almost total inhibition of cell death was obtained employing z-IETD-FMK.

These results suggest that both apoptotic pathways, the intrinsic and the extrinsic, may be triggered by Mn in C6 cells. Even more, these data implicate caspase-8 as the apical caspase of the caspases cascade.

To more thoroughly evaluate the participation of the extrinsic pathway, we examined the effect of Mn exposure on the Fas receptor ligand (FasL) levels by Western Blot analysis. Fig. 4A shows that FasL was expressed at similar levels in control cells both in the presence and absence of serum. Mn exposure increased FasL levels 58 ± 6% and 170 ± 14%, in S and SF, respectively.

Caspase-8 plays an essential role in apoptosis induced by Fas activation. It was also demonstrated that caspase-8 can be processed and activated in response to Mn in lymphoma BL41 cells (El Mchichi et al., 2007). Taking into account these considerations, we verified whether Mn could activate caspase-8 (Fig. 4B). Upon Mn treatment, full length caspase-8, which exists in two isoforms of 53 and 55 kDa, was cleaved into p43 and p41 intermediate fragments. Mn induced an increase in p41/43 kDa levels (125 ± 6%) and a significant decrease in the proforms levels (63 ± 7%). To further demonstrate caspase-8 activation, nuclear morphology and PARP-1 cleavage were analyzed in the presence z-IETD-FMK. As shown in Fig. 4C and D, the preincubation with z-IETD-FMK (10 μM) almost completely prevented both the appearance of apoptotic nuclei and PARP-1 cleavage.

It has been reported that Bid, a BH3 domain–containing pro-apoptotic Bcl-2 family member, is a specific proximal substrate of caspase-8 in the Fas apoptotic signaling pathway. The product of Bid cleavage, truncated Bid (tBid), interacts with other Bcl-2 family members on the mitochondrial surface, which results in mitochondrial outer membrane permeabilization (MOMP) (Chipuk et al., 2010). In this way, caspase-8 engages the mitochondrial pathway to amplify the death signal and execute apoptosis. Western blotting from total lysate extracted from Mn-treated C6 cells confirmed the Bid cleavage in our experimental model revealed by a complete disappearance of the 22 kDa form in cells exposure to Mn in the absence of serum (Fig. 4D). In contrast, Bid expression did not change after the addition of Mn to serum-containing medium (data not shown).

Altogether these data show that Mn activates caspase-8 and Bid cleavage probably compromising the Fas death receptor pathway.

3.6. Apoptosis triggered by Mn involves the mitochondrial apoptotic pathway

Once the functionality of the caspase-8-dependent apoptotic pathway was established, we extended the study to explore the role of the intrinsic pathway.

We have previously demonstrated that caspase-9 specific inhibitor protect C6 cells against death (Supplementary Fig. 2). To further confirm caspase-9 activation, we performed Western Blots employing an anti-caspase polyclonal antibody, which recognizes the 47 kDa form of the enzyme (Fig. 5A). Mn exposure not only produced a marked decrease in the 47 kDa signal at 24 h, but a nearly complete disappearance after 48 h incubation. These results give further support to our evidence involving caspase-9 in C6 cells Mn-induced apoptosis.

One of the rate-limiting steps in apoptotic cell death is the increase in the permeability of the inner/or outer mitochondrial membrane, accompanied by the release of pro-apoptotic factors, such as cytochrome c, which are normally confined to the inner mitochondrial membrane and intermembrane space (Chipuk et al., 2010). In response to apoptotic signals, cytochrome c, apoptotic protease activating factor-1 (APAF-1) and caspase-9 form the apoptosome, a multi-protein complex that functions to activate effector caspases-3 and -7. In order to gain more insight into the triggering of the apoptotic mitochondrial pathway in our model, we studied cytochrome c subcellular localization in cells exposed to Mn. Western blotting from enriched-mitochondrial and cytosolic fractions isolated from Mn-treated cells under SF condition, showed that cytochrome c release from the mitochondria was nearly complete (87 ± 3%)(Fig. 5B). Consequently, a 5.2-fold increase in the cytosolic accumulation of cytochrome c was observed. No significant effect was observed under serum deprivation or Mn exposure in the presence of serum.

Opening of the mitochondrial permeability transition pore (MPTP) has been shown to occur in cellular culture models of neurodegenerative disorders (Sims, 1990; Varbiro et al., 2001) in response to different stressors (Sims, 1990). We therefore tested whether the opening of the MPTP may contribute to apoptotic cell death by employing cyclosporin A (CsA), an inhibitor of cyclophilin D that prevents opening of the pore and thereby depolarization (Broekemeier et al., 1989; Prabhakaran et al., 2009). Preincubation with 1 μM of CsA prevented 35 ± 2% of the cell viability loss induced by Mn (Fig. 5C). These results indicate that the opening of MPTP is involved in the cytotoxic effects displayed by Mn on mitochondria. However, the relatively low recovery obtained in cell viability, suggests that alternative mechanisms participate in the mitochondrial injury.

The Bcl-2 family proteins are known to be involved in the regulation of the apoptotic cell death. Bcl-2 is an anti-apoptotic member predominantly localized in mitochondria that regulates mitochondrial membrane integrity and cytochrome c release. Pro-apoptotic members, such as Bax, mainly reside in the cytoplasm and redistribute into mitochondria in response to death stimuli. Bcl-2 family proteins are able to undergo homodimerization and heterodimerization, and the ratio of pro- to anti-apoptotic proteins determines the fate of cells (Chipuk et al., 2010; Galluzzi et al., 2009).

To reveal the involvement of Bcl-2 family proteins in Mn-induced mitochondrial pathway, we analyzed Bcl-2 and Bax expression in total lysates and enriched-mitochondrial and cytosolic fractions extracted from Mn-treated cells, both in the presence and absence of serum (Supplementary Fig. 3 and Fig. 5D). Mn exposure increased total Bax levels (33 ± 6%) and diminished total Bcl-2 expression (49 ± 9%) compared with their respective controls (Supplementary Fig. 3). When the subcellular fractions were analyzed, a marked increase in mitochondrial Bax and Bcl-2 levels was observed (4.3- and 5.0-fold, respectively). This was accompanied by a decrease of 50% in Bax levels and a nearly complete disappearance of Bcl-2 expression in cytosolic fractions. The MW corresponding to the mitochondrial Bcl-2 signal was found to be lower than those of the cytosol (23 and 26 kDa, respectively). Accordingly, it has been reported that Bcl-2 could be cleaved by caspases under apoptotic stimuli (Cheng et al., 1997). This cleavage results in the loss of the NH2-terminal BH4 homology domain which could inactivate its anti-apoptotic activity or even convert Bcl-2 to a Bax-like effector with pro-apoptotic activity.

Altogether these data demonstrate that the mitochondrial apoptotic pathway plays a relevant role in the Mn-induced apoptosis in C6 cells.

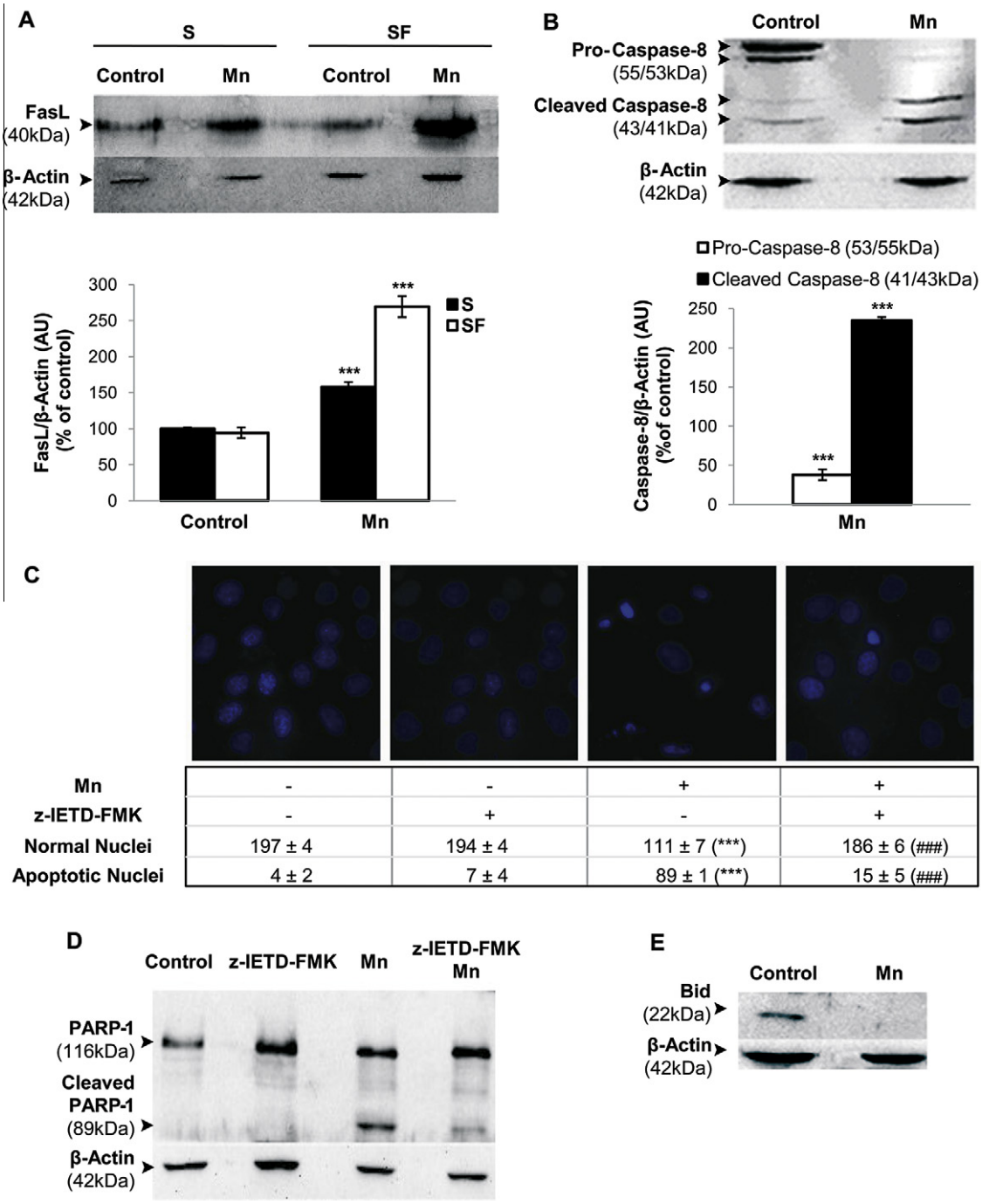

Fig. 4. Mn-induced apoptosis involves caspase-8 activation and Bid cleavage. C6 cells were treated with 750 μM $MnCl_2$ for 24 h. Cell lysates were subjected to immunoblotting analysis employing specific antibodies. Signals were quantified with the ImageJ software. Image corresponds to one representative experiment ($n = 3$). (A) Mn increase FasL (CD95) expression. Results are expressed as a percentage of the serum control considered as 100%. (B) Caspase-8 activation. Results are expressed as a percentage of the respective control considered as 100%. (C-D) z-IETD-FMK inhibits apoptotic events. Cells were pre-incubated with 10 μM of caspase-8 inhibitor (z-IETD-FMK). (C) Nuclear morphology was visualized by fluorescence microscopy after staining with Hoechst 33258. The number of cells with apoptotic morphology was scored (200 cells per sample). Magnification: 1000×. (D) z-IETD-FMK prevented PARP-1 cleavage (50%). (E) Bid is involved in Mn-induced apoptosis. A polyclonal antibody that recognizes Bid protein (full length: 22 kDa) was used for inmunoblotting analysis. (B–D) Experiments were carried out under serum deprivation. Statistically significant differences between the controls and experimental groups are indicated by: $^{***}p < 0.001$ vs. respective control; $^{\#\#\#}p < 0{,}001$ vs. Mn. S: serum; SF: serum free; AU: arbitrary units.

3.7. Mn induces $\Delta\varphi_m$ dissipation and mitochondrial network fragmentation

In a widely accepted model, additional pathways downstream of Bcl-2 proteins such as mitochondrial fragmentation and cristae remodeling, ensure complete release of cytochrome c and mitochondrial dysfunction. Numerous studies have provided compelling evidence that these processes play a causative role in the apoptotic cell death and neurodegeneration (Su et al., 2010). Additionally, a correlation between the mitochondrial transmembrane potential ($\Delta\varphi_m$) dissipation and the mitochondrial network fragmentation has been established (Legros et al., 2002).

The potential effects of Mn on mitochondrial integrity were analyzed by fluorescence microscopy employing MitoTracker Red

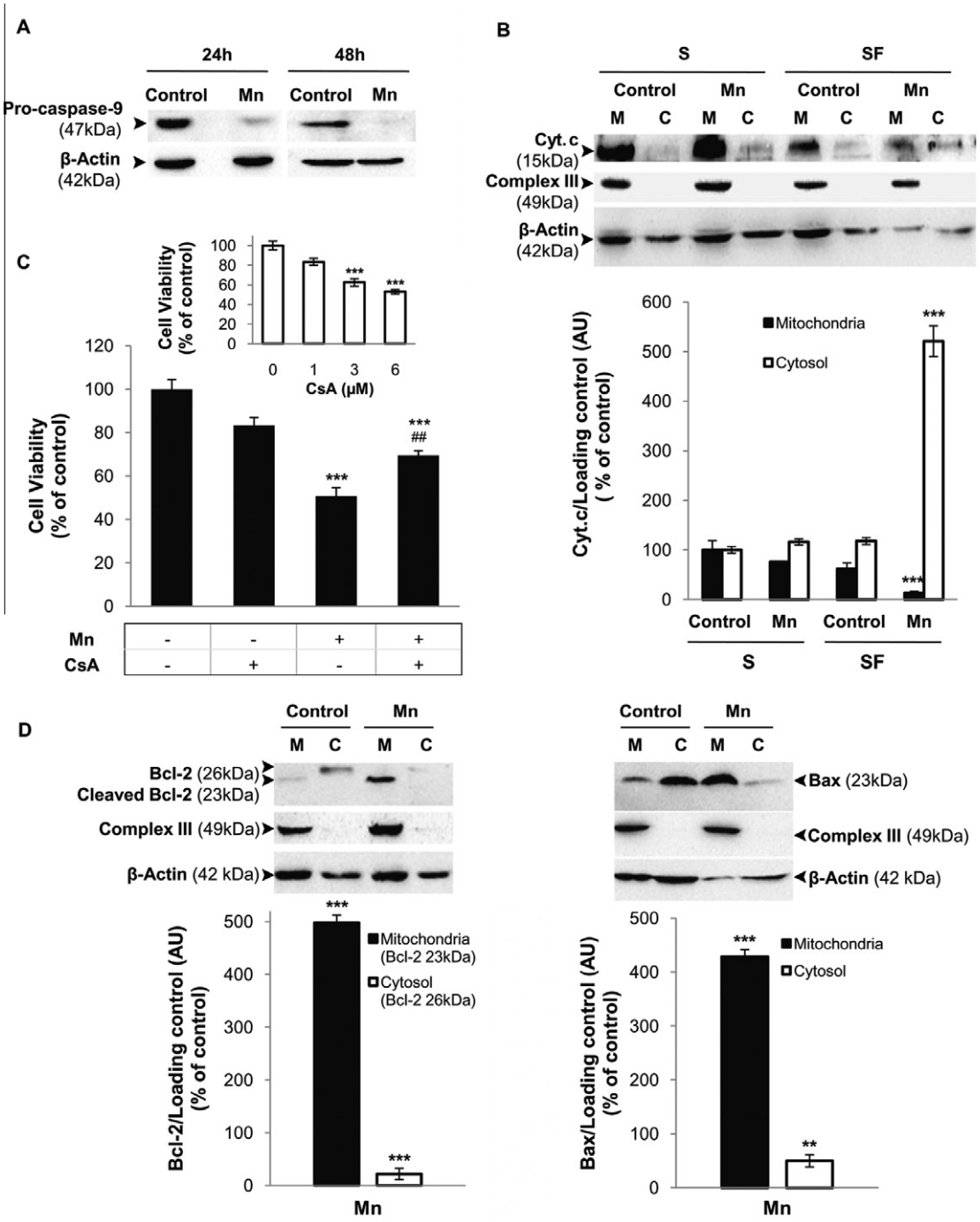

Fig. 5. Mn triggers mitochondrial apoptotic pathway. (A) Caspase-9 activation. Cell lysates from 24 and 48 h Mn treatment were subjected to immunoblotting procedure employing a polyclonal antibody that recognizes caspase-9. Blots were reprobed with β-Actin antibody to normalize for protein loading. (B) Cytochrome c release. C6 cells were incubated with 750 μM Mn for 24 h in either the absence (SF) or presence (S) of serum. Enriched-mitochondrial and cytosolic fractions were subjected to immunoblotting procedure using an antibody that recognizes cytochrome c protein. Reprobing with a complex III subunit core 1-OxPhos (complex III) and β-actin antibodies was performed to normalize for loading control. (C) Mitochondrial permeability transition pore (MPTP) blockage. Cells were pre-incubated with 1 μM Ciclosporine (CsA) and MTT assay was performed. Inset: dose-response curve to determine the optimal CsA concentration based on cell viability measured by MTT assay. (D) Role of Bcl-2 family proteins in Mn-induced apoptosis. Mitochondrial and cytosolic fractions were subjected to immunoblotting procedure using antibodies that recognize Bcl-2 (left) and Bax (right) proteins. Results are expressed as a percentage of the respective control considered as 100%. (A, C and D): Experiments were carried out under serum deprivation. Statistically significant differences between the controls and experimental groups are indicated by: $^{**}p < 0.01$, $^{***}p < 0.001$ vs. control and $^{\#\#}p < 0.01$ vs. Mn. AU: arbitrary units; cyt. c: cytochrome c.

CMXRos, a red-fluorescent dye that stains mitochondria in living cells being its accumulation dependent on membrane potential.

Mitochondrial morphology was classified into three categories: tubular (normal), intermediate (tubular with swollen regions) and fragmented (small and globular) (Fig. 6). In control cells, mitochondria were distributed in the cell somata and the cellular processes, mostly exhibiting the expected tubular morphology. In contrast, under SF conditions, Mn-treated cells exhibited an increase in the amount of intermediate and fragmented mitochondria, localized mainly as perinuclear aggregates (Fig. 6) which

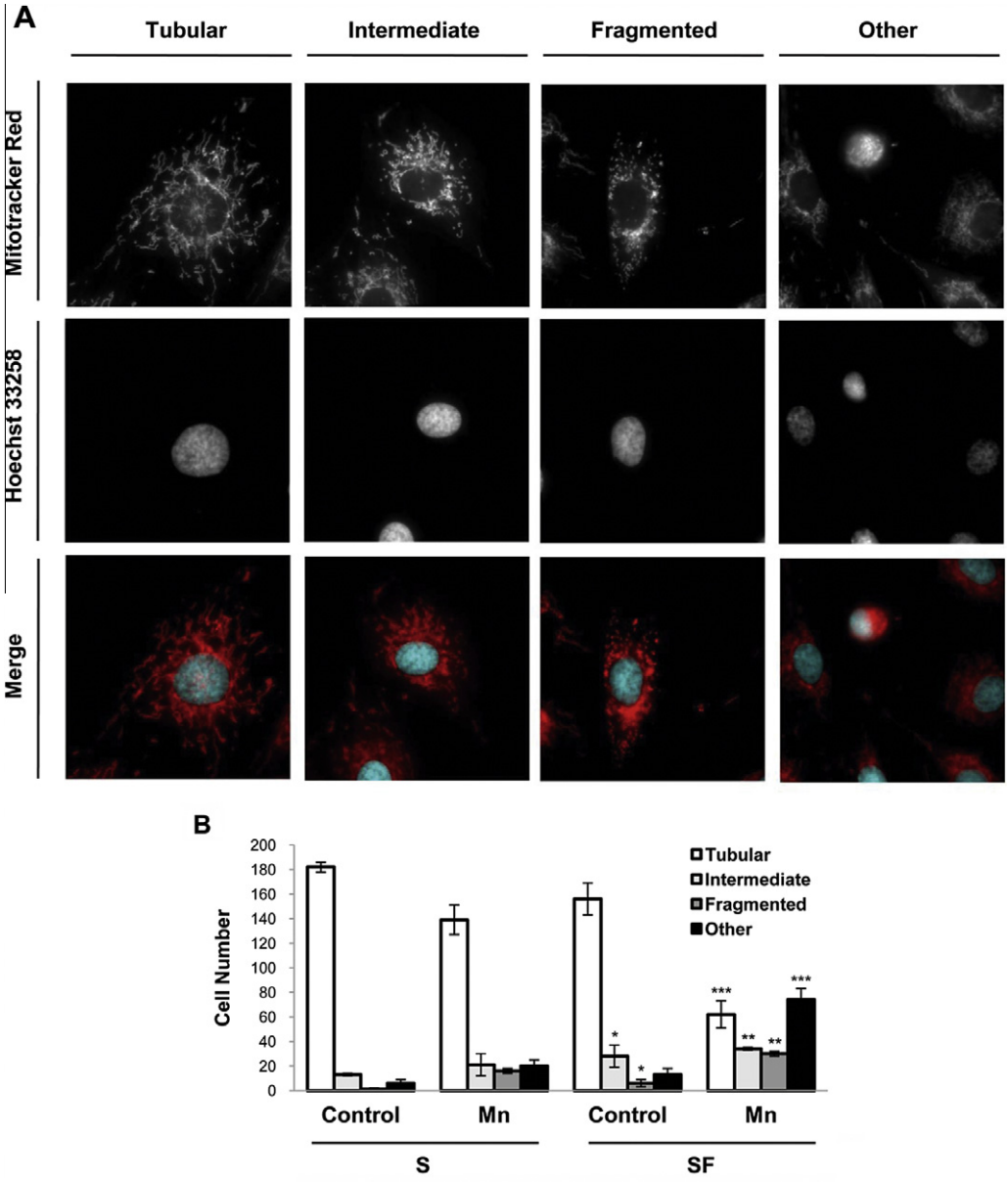

Fig. 6. Mn-induced $\Delta\varphi_m$ dissipation and mitochondrial network collapse. (A) Mitochondria were visualized with 75 nM MitoTracker Red CMXRos by fluorescence microscopy (TRITC Filter. λ_{ex}: 528–553 nm; λ_{em}: 600–660 nm) (magnification: 600×). Three cell categories exhibiting different mitochondrial morphology were classified: tubular (normal), intermediate (filamentous with swollen regions) and fragmented (small and globular). Cells classified as "Other" refers to those exhibiting nuclear condensation and $\Delta\psi_m$ collapse (upper panel). Nuclear DNA was stained with Hoechst 33258 dye and visualized by fluorescence microscopy using filters for DAPI (λ_{ex}: 330–380 nm; λ_{em}: 435–485 nm) (Middle panel). Red (mitochondria) and cyan (nuclei) images were merged (lower panel). (B) 200 cells/sample were scored and classified according to item A. Two independent experiments were conducted. Statistically significant differences between the controls and experimental groups are indicated by: $^{*}p < 0.05$, $^{**}p < 0.01$, $^{***}p < 0.001$ vs. control. S: serum; SF: serum free. (For interpretation of the references to color in this figure legend, the reader is referred to the web version of this article.)

agrees with Sheridan and Martin (2010). In addition, a 7.4-fold increase of cells undergoing nuclear condensation and $\Delta\varphi_m$ collapse, events consistent with the apoptotic cell death, was observed (Fig. 6, panel "Other"). Altogether, these results indicate that Mn induced the loss of the mitochondrial integrity by increasing the $\Delta\varphi_m$ dissipation and the mitochondrial fragmentation.

4. Discussion

It is well known that astrocytes serve as the major homeostatic regulator and storage site for Mn in the brain (Aschner et al., 1999). However, Mn accumulation in astroglia may interfere with their normal functions leading to an increased release of various proinflammatory and neurotoxic cytokines as well as free radicals that ultimately may exert deleterious effect on neurons (Zhang et al., 2009). In addition, astrocytes themselves may be induced to die by apoptosis (Gonzalez et al., 2008). In spite of the considerable knowledge gained on the role of the astroglia in Mn-induced neurotoxicity, there is still little understanding about the detailed signaling cascades underlying the mechanisms of Mn-induced apoptosis in astrocytes.

In the present study we used the rat astrocytoma C6 cells as an *in vitro* model system to more thoroughly characterize the molecular pathways involved in Mn-induced apoptosis. C6 cells, due to its capacity to retain normal glial cell properties, have been

considered as an appropriate experimental model for studying cellular and molecular mechanisms involved on heavy metal neurotoxicity (Prasad, 1983).

Our results show that C6 cells are sensitive to Mn exposure. In fact, the MTT and NR assays showed a significant dose-dependent decrease in cell viability (Fig. 1) accompanied by cells exhibiting morphological changes consistent with apoptotic cell death (Supplementary Fig. 1). Interestingly, for all the tested concentrations, cell viability measured by NR assay was lower than the corresponding values obtained by MTT assay. These results suggest a higher susceptibility of the lysosomes towards Mn than those of the mitochondria. Accordingly, our group has described the involvement of a lysosomal pathway in C6 cells exposed to Mn for 6 h (Gorojod et al., 2009, 2010).

Mn-induced apoptosis has been described in different cell types (Desole et al., 1997; El Mchichi et al., 2007; Oubrahim et al., 2001; Roth et al., 2000; Schrantz et al., 1999; Tamm et al., 2008) including rat cortical astrocytes (Gonzalez et al., 2008; Yin et al., 2008). In this report, we demonstrate that the type of cell death induced by Mn is predominantly apoptotic, as determined by Hoechst 33258 staining, caspase-3 activation and PARP-1 cleavage (Fig. 3). In addition, these data provide evidence supporting the fact that apoptotic cell death occurs through a caspase-dependent-pathway.

Oxidative stress has been implicated as a contributing mechanism by which Mn mediates its cytotoxic effects. It has been proposed that through its sequestration in mitochondria, Mn interferes with proper respiration, thereby leading to excessive ROS production (Galvani et al., 1995). Herein, we demonstrate that Mn induces ROS generation in a dose-dependent manner in accordance with our previous results (Gonzalez et al., 2008) (Fig. 2A). Furthermore pre-incubations with potent antioxidants such as GSH, NAC, ASA and MLT were proved to prevent Mn-induced decrease in cell viability (Fig. 2B). These results provide evidence for the involvement of oxidative stress in the onset of apoptotic cell death.

Previous reports have indicated that the signaling system Fas/CD95R and its ligand FasL are expressed in human and rat brains in both normal and tumoral tissues. In particular, C6 rat astrocytoma cells express high levels of FasL (Saas et al., 1997). This signaling system has been described in Alzheimer's and Parkinson's disease (Erten-Lyons et al., 2010; Pan et al., 2007). Based on this background and taking into account the fact that Mn accumulation in the brain leads to Parkinson's type disease, we studied the possible participation of this receptor pathway in our Mn-induced Parkinsonism model. Results shown in Fig. 4A, B and E demonstrated that Mn increases FasL levels, caspase-8 activation and Bid cleavage. Consistently with these data, the preincubation with the specific inhibitor of caspase-8, z-IETD-FMK, almost completely prevented cell death, as well as PARP-1 cleavage and the appearance of apoptotic nuclei (Supplementary Fig. 2, Fig. 4C and D). These results strongly support the involvement of a functional caspase-8-dependent pathway in Mn-induced apoptosis.

Caspase-8 can activate caspase-3 through different signaling pathways, either directly (Type I) or through mitochondria (Type II), depending on the level of caspase-8 activation upon the death-inducing signaling complex (DISC) (Scaffidi et al., 1998). The transition from the extrinsic to the intrinsic pathway is achieved through the Bid processing mediated by caspase-8. Therefore, our results suggest that the death receptor apoptotic pathway could be functional in our experimental model.

Numerous studies have reported difficulty in detecting active caspase-8 (p43-p10) at the DISC in type II cells. These results and recent evidence demonstrating that after Fas activation, p43-p10 caspase-8 is readily detectable on the mitochondrial membrane in diverse cell lines (Schug et al., 2011) would question our suggestion about the functionality of the receptor pathway in our model. Nevertheless, Schug et al. (2011) speculated that p43-p10 is formed at the DISC and is subsequently translocated to the mitochondria, supporting our hypothesis that caspase-8 is activated in the DISC, triggering the death signal. However, we can not exclude the possibility that caspase-8 would be activated by a lysosomal pathway, according to Baumgartner et al. (2007) and Gorojod et al. (2010). El Mchichi et al. (2007) have reported that p38 MAPK and MSK1 could mediate caspase-8 activation in lymphoma B cells. Therefore, the precise pathway responsible for caspase-8 activation under our experimental conditions is not yet defined and needs further investigations.

Mn neurotoxicity has been associated with mitochondrial dysfunction in neuronal and glial cell lines. Mn inhibits oxidative phosphorylation and mitochondrial complex I in PC12 cells (Galvani et al., 1995) and disrupts the mitochondrial membrane potential in cultured astrocytes (Barhoumi et al., 2004; Gonzalez et al., 2008; Kakulavarapu et al., 2004; Yin et al., 2008). In addition, it has been established that among the multiple molecular mechanisms shared by Manganism and PD, the mitochondrial dysfunction plays a relevant role (Benedetto et al., 2009). Therefore inhibition of mitochondrial function by Mn may produce neuroanatomic changes and consequent motor dysfunction similar to those observed in PD patients. Taking into account these considerations, we investigated the possibility that Mn may sensitize cells to die by apoptosis by compromising mitochondrial function. Our present data show that Mn induces opening of MPTP, loss of $\Delta\varphi_m$ and the release of cytochrome c from the mitochondria to the cytosol (Fig 5), in agreement with our previous results obtained in primary cortical rat astrocytes (Gonzalez et al., 2008). It is well known that the release of cytochrome c facilitates the formation of the apoptosome-containing adaptor APAF-1 and the initiator caspase-9. Like caspase-8, caspase-9 can directly activate the effector caspase-3. While this serves as an amplification mechanism of cell death, damage to mitochondria and subsequent apoptosome-mediated caspase-9 activation is widely accepted as the initiating event in the intrinsic apoptosis pathway (Green and Reed, 1998). In this report we demonstrate caspase-9 activation and the significant cell death prevention induced by its specific inhibitor (Fig. 5).

Even more, Mn induced a dramatic increase in mitochondrial Bax and Bcl-2 signals. Previous findings have indicated that under specific apoptotic stimuli, anti-apoptotic Bcl-2 family members can be cleaved and thereby converted into pro-apoptotic molecules directly facilitating cytochrome c release (Cheng et al., 1997). Such a mechanism could explain our current observations taking into account that the MW corresponding to the Bcl-2 form resident in mitochondria was 23 kDa, this is the same value reported for the pro-apoptotic cleaved product. Results presented here suggest that Mn shift the total and mitochondrial levels of Bcl-2 and Bax to favor the apoptotic process. Altogether these data are compatible with caspase-dependent mitochondrial apoptotic pathway being functional in C6 cells Mn-induced apoptosis.

Mitochondria are morphologically dynamic organelles that continuously undergo fission and fusion to form small individual units or interconnected networks (Sheridan and Martin, 2010). During apoptosis, the mitochondrial network fragmentation occurs, resulting in smaller and more numerous mitochondria. This phenotype is often found upstream of caspase activation and close to Bax translocation to the mitochondria and cytochrome c release, suggesting a mechanistic link between mitochondrial morphology changes and apoptosis. As far as we know there are no studies describing these processes in Mn-treated cells undergoing apoptosis. Our findings showed that in Mn-treated cells mitochondria exhibited a mixture of tubular and rounded morphologies and tended to be more aggregated in the perinuclear space. In addition, a marked increase in the number of cells undergoing apoptotic events was observed (Fig. 6, "Other" Panel). Although our results

confirm previous reports indicating that Mn induces loss of $\Delta\varphi_m$, in this report we go deeper by demonstrating the involvement of mitochondrial fragmentation in Mn-induced apoptosis in C6 cells.

On the other hand, our studies comparing different parameters both in the presence and absence of serum demonstrated that serum deprivation by itself has no effect, confirming the fact that all the changes observed exclusively reflect the Mn action.

5. Conclusions

In summary, our results provide a novel explanation for the molecular mechanism involved in Mn-induced apoptosis in C6 cells. Firstly, at least two functional pathways are triggered by Mn; the mitochondrial pathway and a caspase-8 dependent pathway. Secondly, Mn induces changes in Bax and Bcl-2 mitochondrial levels to favor the apoptotic demise. Finally, in addition to produce $\Delta\varphi_m$ dissipation, Mn induces an imbalance in fusion/fission equilibrium resulting in an enhancement of mitochondrial fragmentation.

These results represent a relevant contribution to the understanding of the mechanisms by which astrocytoma C6 cells undergo apoptotic cell death and will be helpful to the purpose of designing novel molecular intervention targets in Manganism and perhaps Parkinson disease.

Acknowledgments

This work was supported by Consejo Nacional de Investigaciones Científicas y Técnicas, CONICET (PIP Nos. 02631 and 5406). The authors thank Dr. Elizabeth Jares-Erijman and Francisco Guaimas from the Organic Chemistry Department, FCEN-UBA, for their excellent assistance in obtaining fluorescence microscopy images. The authors are very grateful to Dr. Elba Vazquez for the critical reading of the manuscript. We acknowledge the contribution of Dr. Mónica Costas for providing Bid primary antibody and Dr. Pablo Mele from the Human Medicine Department, Faculty of Medicine, UBA for providing the OxPhos (Complex III) primary antibody. A.A and R.M.G. thanks CONICET for a studentship. M.L.K. is research member of CONICET.

Appendix A. Supplementary data

Supplementary data associated with this article can be found, in the online version, at doi:10.1016/j.neuint.2011.06.001.

References

Aschner, M., Guilarte, T.R., Schneider, J.S., Zheng, W., 2007. Manganese: recent advances in understanding its transport and neurotoxicity. Toxicol. Appl. Pharmacol. 221, 131–147.

Aschner, M., Vrana, K.E., Zheng, W., 1999. Manganese uptake and distribution in the central nervous system (CNS). Neurotoxicology 20, 173–180.

Barhoumi, R., Faske, J., Liu, X., Tjalkens, B., 2004. Manganese potentiates lipopolysaccharide-induced expression of NOS2 in C6 glioma cells through mitochondrial-dependent activation of nuclear factor kappaB. Mol. Brain Res. 122, 167–179.

Baumgartner, H.K., Gerasimenko, J.V., Thorne, C., Ashurst, L.H., Barrow, S.L., Chvanov, M.A., Gillies, S., Criddle, D.N., Tepikin, A.V., Petersen, O.H., Sutton, R., Watson, A.J.M., Gerasimenko, O.V., 2007. Caspase-8-mediated apoptosis induced by oxidative stress is independent of the intrinsic pathway and dependent on cathepsins. Am. J. Physiol. Gastrointest. Liver Physiol. 293, G296–G307.

Benda, P., Lightbody, J., Sato, G., Levine, L., Sweet, W., 1968. Differentiated rat glial cell strain in tissue culture. Science 161, 370–371.

Benedetto, A., Au, C., Aschner, M., 2009. Manganese-induced dopaminergic neurodegeneration: insights into mechanisms and genetics shared with Parkinson Disease. Chem. Rev. 109, 4862–4884.

Borenfreund, E., Puerner, J.A., 1985. Toxicity determined in vitro by morphological alterations and neutral red absorption. Toxicol. Lett. 24, 119–124.

Bradford, M.M., 1976. A rapid and sensitive method for the quantitation of microgram quantities of protein utilizing the principle of protein–dye binding. Anal. Biochem. 72, 248–254.

Broekemeier, K.M., Dempsey, M.E., Pfeiffer, D.R., 1989. Cyclosporin A is a potent inhibitor of the inner membrane permeability transition in liver mitochondria. J. Biol. Chem. 264, 7826–7830.

Budihardjo, I., Oliver, H., Lutter, M., Luo, X., Wang, X., 1999. Biochemical pathways of caspase activation during apoptosis. Annu. Rev. Cell Dev. Biol. 15, 269–290.

Chen, C., Liao, S., 2002. Oxidative stress involves in astrocytic alterations induced by manganese. Exp. Neurol. 175, 216–225.

Cheng, E.H., Kirsch, D.G., Clem, R.J., Ravi, R., Kastan, M.B., Bedi, A., Ueno, K., Hardwick, J.M., 1997. Conversion of Bcl-2 to a Bax-like death effector by caspases. Science 278, 1966–1968.

Chipuk, J.E., Moldoveanu, T., Llambi, F., Parsons, M.J., Green, D.R., 2010. The Bcl-2 family reunion. Mol. Cell 37, 299–310.

Desole, M.S., Sciola, L., Delogu, M.R., Sircana, S., Migheli, R., Miele, E., 1997. Role of oxidative stress in the manganese and 1-methyl-4-(2′-ethylphenyl)-1,2,3,6-tetrahydropyridine-induced apoptosis in PC12 cells. Neurochem. Int. 31, 169–176.

Dorman, D.C., Struve, M.F., Marshall, M.W., Parkinson, C.U., James, R.A., Wong, B.A., 2006. Tissue manganese concentrations in young male rhesus monkeys following subchronic manganese sulfate inhalation. Toxicol. Sci. 92, 201–210.

El Mchichi, B., Hadji, A., Vazquez, A., Leca, G., 2007. P38 MAPK and MSK1 mediate caspase-8 activation in manganese-induced mitochondria-dependent cell death. Cell Death Diff. 14, 1826–1836.

Erten-Lyons, D., Jacobson, A., Kramer, P., Grupe, A., Kaye, J., 2010. The FAS gene, brain volume, and disease progression in Alzheimer's disease. Alzheimers Dement. 6, 118–124.

Galluzzi, L., Blomgren, K., Kroemer, G., 2009. Mitochondrial membrane permeabilization in neuronal injury. Nat. Rev. Neurosci. 10, 481–494.

Galvani, P., Fumagalli, P., Santagostino, A., 1995. Vulnerability of mitochondrial complex I in PC12 cells exposed to manganese. Eur. J. Pharmacol. 293, 377–383.

Gonzalez, L.E., Juknat, A.A., Venosa, A.J., Verrengia, N., Kotler, M.L., 2008. Manganese activates the mitochondrial apoptotic pathway in rat astrocytes by modulating the expression of proteins of the Bcl-2 family. Neurochem. Int. 53, 408–415.

Gorojod, R.M., Alaimo, A., Sapienza, C., Kotler, M.L., 2009. Role of the lysosomal pathway in Mn-induced cell death in C6 glioma cells. Medicina 69 (Suppl. 1), 242 (abstract).

Gorojod, R.M., Alaimo, A., Sapienza, C., Kotler, M.L., 2010. A lysosomal-autophagic pathway is involved in Mn-induced cellular damage. Medicina 70 (Suppl. 2), 163 (abstract).

Green, D.R., Reed, J.C., 1998. Mitochondria and apoptosis. Science 281, 1309–1312.

Gunter, T.E., Gavin, C.E., Aschner, M., Gunter, K.K., 2006. Speciation of manganese in cells and mitochondria: a search for the proximal cause of manganese toxicity. Neurotoxicology 27, 765–776.

Hirata, Y., 2002. Manganese-induced apoptosis in PC12 cells. Neurotoxicol. Teratol. 24, 639–653.

Ito, Y., Oh-Hashi, K., Kiuchi, K., Hirata, Y., 2006. P44/42 MAP kinase and c-Jun N-terminal kinase contribute to the up-regulation of caspase-3 in manganese-induced apoptosis in PC12 cells. Brain Res. 1099, 1–7.

Kakulavarapu, V., Rao, R., Noremberg, M.D., 2004. Manganese induces the mitochondrial permeability transition in cultured astrocytes. J. Biol. Chem. 279, 32333–32338.

Kotler, M.L., Gonzalez, L.E., Cortina, M.E., Juknat, A.A., 2005. Astrocytes fate: oxidative stress versus HO1/MAPK. Biocell 29 (Suppl.), 109 (Abstract).

Legros, F., Lombes, A., Frachon, P., Rojo, M., 2002. Mitochondrial fusion in human cells is efficient, requires the inner membrane potential, and is mediated by mitofusins. Mol. Biol. Cell 13, 4343–4354.

Li, Y., Sun, L., Cai, T., Zhang, Y., Lv, S., Wang, Y., Ye, L., 2010. Alpha-Synuclein overexpression during manganese-induced apoptosis in SH-SY5Y neuroblastoma cells. Brain Res. Bull. 81, 428–433.

Liu, X., Buffington, J.A., Tjalkens, R.B., 2005. NF-κB-dependent production of nitric oxide by astrocytes mediates apoptosis in differentiated PC12 neurons following exposure to manganese and cytokines. Mol. Brain Res. 141, 39–47.

Martín, V., Herrera, F., Carrera-Gonzalez, P., García-Santos, G., Antolín, I., Rodriguez-Blanco, J., Rodríguez, C., 2006. Intracellular signaling pathways involved in the cell growth inhibition of glioma cells by melatonin. Cancer Res. 66, 1081–1088.

Milatovic, D., Yin, Z., Gupta, R.C., Sidoryk, M., Albrecht, J., Aschner, J.L., Aschner, M., 2007. Manganese induces oxidative impairment in cultured rat astrocytes. Toxicol. Sci. 98, 198–205.

Mosmann, T., 1983. Rapid colorimetric assay for cellular growth and survival: application to proliferation and cytotoxicity assays. J. Immunol. Methods 65, 55–63.

Nedergaard, M., Ransom, B., Goldman, S.A., 2003. New roles for astrocytes: redefining the functional architecture of the brain. Trends Neurosci. 26, 523–530.

Oubrahim, H., Chock, P.B., Stadtman, E.R., 2002. Manganese(II) induces apoptotic cell death in NIH3T3 cells via a caspase-12-dependent pathway. J. Biol. Chem. 277, 20135–20138.

Oubrahim, H., Stadtman, E.R., Boon Chock, P., 2001. Mitochondria play no roles in Mn(II)-induced apoptosis in HeLa cells. Proc. Natl. Acad. Sci. USA 98, 9505–9510.

Pan, J., Zhao, Y.X., Wang, Z.Q., Jin, L., Sun, Z.K., Chen, S.D., 2007. Expression of FasL and its interaction with Fas are mediated by c-Jun N-terminal kinase (JNK) pathway in 6-OHDA-induced rat model of Parkinson disease. Neurosci. Lett. 428, 82–87.

Prabhakaran, K., Chapman, G.D., Gunasekar, P.G., 2009. BNIP3 up-regulation and mitochondrial dysfunction in manganese-induced neurotoxicity. Neurotoxicology 30, 414–422.

Prasad, K.N., 1983. Use of cultures of neuroblastoma and glioma as a model system to study the heavy metal-induced neurotoxicity. In: Kobler, A.R., Wong, T.K., Grant, R.S., de Woskin, R.S., Hughes, T.J. (Eds.), In Vitro Toxicity Testing of Environmental Agents, Current and Future Possibilities. Part A. Plenum Press, New York, pp. 421–472.

Roth, J.A., 2009. Are there common biochemical and molecular mechanisms controlling Manganism and Parkisonism. Neuromol. Med. 11, 281–296.

Roth, J.A., Feng, L., Walowitz, J., Browne, R.W., 2000. Manganese-induced rat pheochromocytoma (PC12) cell death is independent of caspase activation. J. Neurosci. Res. 61, 162–171.

Saas, P., Walker, P.R., Hahne, M., Quiquerez, A.L., Schnuriger, V., Perrin, G., French, L., Van Meir, E.G., de Tribolet, N., Tschopp, J., Dietrich, P.Y., 1997. Fas ligand expression by astrocytoma in vivo: maintaining immune privilege in the brain? J. Clin. Invest. 99, 1173–1178.

Scaffidi, C., Fulda, S., Srinivasan, A., Friesen, C., Li, F., Tomaselli, K.J., Debatin, K.M., Krammer, P.H., Peter, M.E., 1998. Two CD95 (APO-1/Fas) signaling pathways. EMBO J. 17, 1675–1687.

Schrantz, N., Blanchard, D.A., Mitenne, F., Auffredou, M.T., Vazquez, A., Leca, G., 1999. Manganese induces apoptosis of human B cells: caspase-dependent cell death blocked by bcl-2. Cell Death Differ. 6, 445–453.

Schug, Z.T., Gonzalvez, F., Houtkooper, R.H., Vaz, F.M., Gottlieb, E., 2011. BID is cleaved by caspase-8 within a native complex on the mitochondrial membrane. Cell Death Differ. 18, 538–548.

Sheridan, C., Martin, S.J., 2010. Mitochondrial fission/fusion dynamics and apoptosis. Mitochondrion 10, 640–648.

Sims, N.R., 1990. Rapid isolation of metabolically active mitochondria from rat brain and subregions using Percoll density gradient centrifugation. J. Neurochem. 55, 698–707.

Su, B., Wang, X., Zheng, L., Perry, G., Smith, M.A., Zhu, X., 2010. Abnormal mitochondrial dynamics and neurodegenerative diseases. Biochim. Biophys. Acta 1802, 135–142.

Tamm, C., Sabri, F., Ceccatelli, S., 2008. Mitochondrial-mediated apoptosis in neural stem cells exposed to manganese. Toxicol. Sci. 101, 310–320.

Tholey, G., Ledig, M., Mandel, P., Sargentini, L., Frivold, A.H., Leroy, M., Grippo, A.A., Wedler, F.C., 1988. Concentrations of physiologically important metal ions in glial cells cultured from chick cerebral cortex. Neurochem. Res. 13, 45–50.

Varbiro, G., Veres, B., Gallyas Jr., F., Sumegi, B., 2001. Direct effect of Taxol on free radical formation and mitochondrial permeability transition. Free Radic. Biol. Med. 31, 548–558.

Wedler, F.C., Denman, R.B., 1984. Glutamine synthetase: the major Mn(II) enzyme in mammalian brain. Curr. Top. Cell Regul. 24, 153–169.

Yin, Z., Aschner, J.L., dos Santos, A.P., Aschner, M., 2008. Mitochondrial-dependent manganese neurotoxicity in rat primary astrocyte cultures. Brain Res. 1203, 1–11.

Zhang, P., Wong, T.A., Lokuta, K.M., Turner, D.E., Vujisic, K., Liu, B., 2009. Microglia enhance manganese chloride-induced dopaminergic neurodegeneration: role of free radical generation. Exp. Neurol. 217, 219–230.